Accepted Manuscript

Fullerene bisadduct regioisomers containing an asymmetric diamide tether

Tatjana J. Kop, Jelena Đorđević, Mira S. Bjelaković, Dragana Milić

PII: S0040-4020(17)31115-8

DOI: 10.1016/j.tet.2017.10.069

Reference: TET 29072

To appear in: *Tetrahedron*

Received Date: 26 June 2017

Revised Date: 17 October 2017

Accepted Date: 26 October 2017

Please cite this article as: Kop TJ, Đorđević J, Bjelaković MS, Milić D, Fullerene bisadduct regioisomers containing an asymmetric diamide tether, *Tetrahedron* (2017), doi: 10.1016/j.tet.2017.10.069.

Graphical Abstract

Fullerene bisadduct regioisomers containing an asymmetric diamide tether

Leave this area blank for abstract info.

Tatjana J. Kop, Jelena Đorđević, Mira S. Bjelaković, and Dragana R. Milić

University of Belgrade - Institute of Chemistry, Technology and Metallurgy, Center for Chemistry, Njegoševa 12, 11000 Belgrade, Serbia

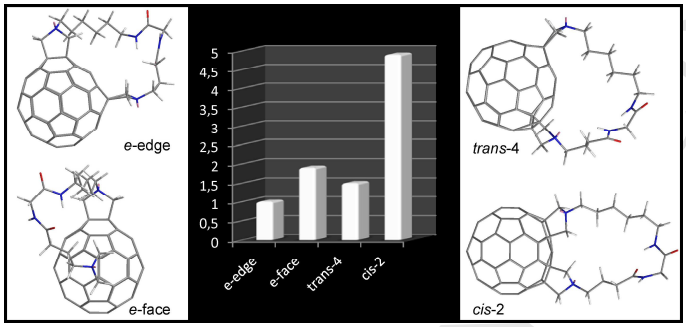

Tetrahedron
journal homepage: www.elsevier.com

Fullerene bisadduct regioisomers containing an asymmetric diamide tether

Tatjana J. Kop[a] , Jelena Đorđević[b], Mira S. Bjelaković[a,] ∗ and Dragana Milić[b]

[a] *University of Belgrade - Institute of Chemistry, Technology and Metallurgy, Center for Chemistry, Njegoševa 12, 11000 Belgrade, Serbia.*
[b] *University of Belgrade - Faculty of Chemistry, Studentski trg 12-16, 11158 Belgrade, Serbia.*

ARTICLE INFO

Article history:
Received
Received in revised form
Accepted
Available online

Keywords:
bis(pyrrolidino)fullerene regioisomers
Prato's cycloaddition
hexamethylene-Gly-Gaba diamide tether
NMR analysis
self-ordering

ABSTRACT

Four macrocyclic bis(pyrrolidino)fullerene regioisomers with *e*-edge, *e*-face, *trans*-4 and *cis*-2 addition patterns were synthesized from the corresponding monoadduct by Prato's cycloaddition in a yield of 50%, and fully characterized by spectroscopic techniques. Bisadduct regioisomers were isolated easily in a pure form using dry-flash column chromatography. The relative ratio of the isolated regioisomers *e*-edge/*e*-face/*trans*-4/*cis*-2 was 1.0:1.9:1.5:4.9. Morphology of self-assembled structures of the four bisadduct regioisomers in solution was characterized using scanning electron microscopy.

1. Introduction

Controlled Bingel–Hirsch, Prato and Diels–Alder biscycloadditions are the most common reactions for the introduction of functional groups to fullerene [6,6]-double bonds and systematic studies on their regiochemistry have become one of the main goals of modern fullerene chemistry. Depending on the addend structure and the applied reaction conditions, biscycloadditions to the C_{60} fullerene sphere by different synthetic procedures can theoretically result in the formation of eight or nine regioisomeric bisadducts, as well as a dumbbell-type derivative.[1] Studies of reactivity and the application of fullerene bisadducts are often hampered by the inefficiency in obtaining pure products from the complex mixtures of regioisomers. So, in many cases bisadducts have been characterized and examined as mixtures of regioisomers,[2] while examples of their successful separation and complete individual characterization are rare.[3] At the same time, it has been demonstrated that the physicochemical properties of single regioisomers showed better photovoltaic performances and higher efficiency as electron acceptors in bulk heterojunction polymer solar cells than those of the corresponding isomer mixtures.[4] This is particularly crucial in materials applications since the self-organization and interaction between molecules is strongly dependent on the molecular structure. Therefore, controlled bisfunctionalization of C_{60} is pivotal not only to improve the yield of the desired bisadduct, but also in the simplification of laborious chromatographic separations. The first attempts of the regioselective synthesis of some bisadducts were based on the reversible introduction of 2,6-dimethoxyanthracene as a directing group for bisadditions to fullerene C_{60} in nucleophilic cyclopropanations. In this way an increased contribution of *cis*-isomers was achieved, but without significant selectivity.[5] The first double cycloaddition to C_{60} directed by the substrate was carried out by combining two cycloadditions, Bingel and Diels-Alder, with regioselective production of the *equatorial* isomer with an excellent yield of 50%.[6] Most of the regioselective syntheses of fullerene bisadducts are now based on tethers with two reactive moieties directing to the desired positions using Bingel,[1c,7] Diels-Alder[1d,4b] and Prato[4a,8,9] cycloaddition reactions. Tether-directed remote multifunctionalization is a widely accepted method for the regio- and stereoselective synthesis of C_{60} multiple adducts, and was extensively investigated in the case of double Bingel cycloadditions, in which two malonate moieties are connected through a xylylene bridge.[1d] Hirsch and co-workers reported a new type of flexible alkyl tether in bis- and tris-malonate macrocycles which gave a completely regioselective reaction with C_{60} and good yields of bisadducts.[10] Most of the known biscycloadditions by Prato's fulleropyrrolidine synthetic methodology use free amino acids and dialdehydes bridged by different structural subunits: crown ethers,[9a] triphenylamine,[9b] a phthalocyanine dimer,[9c] and regioisomeric xylylenes and biphenyls.[9d] A supramolecular-directed functionalization approach was applied, for the first time, for the regio-, stereo-, and atroposelective synthesis of an untethered C_{60} bisadduct with a *cis*-1 addition pattern.[11] The regioselective synthesis of *cis*-1 fullerene bisadducts starting from the commercially available

∗ Corresponding author. +381 11 2635 104; fax: +381 11 2636 061; e-mail: mbjelak@chem.bg.ac.rs

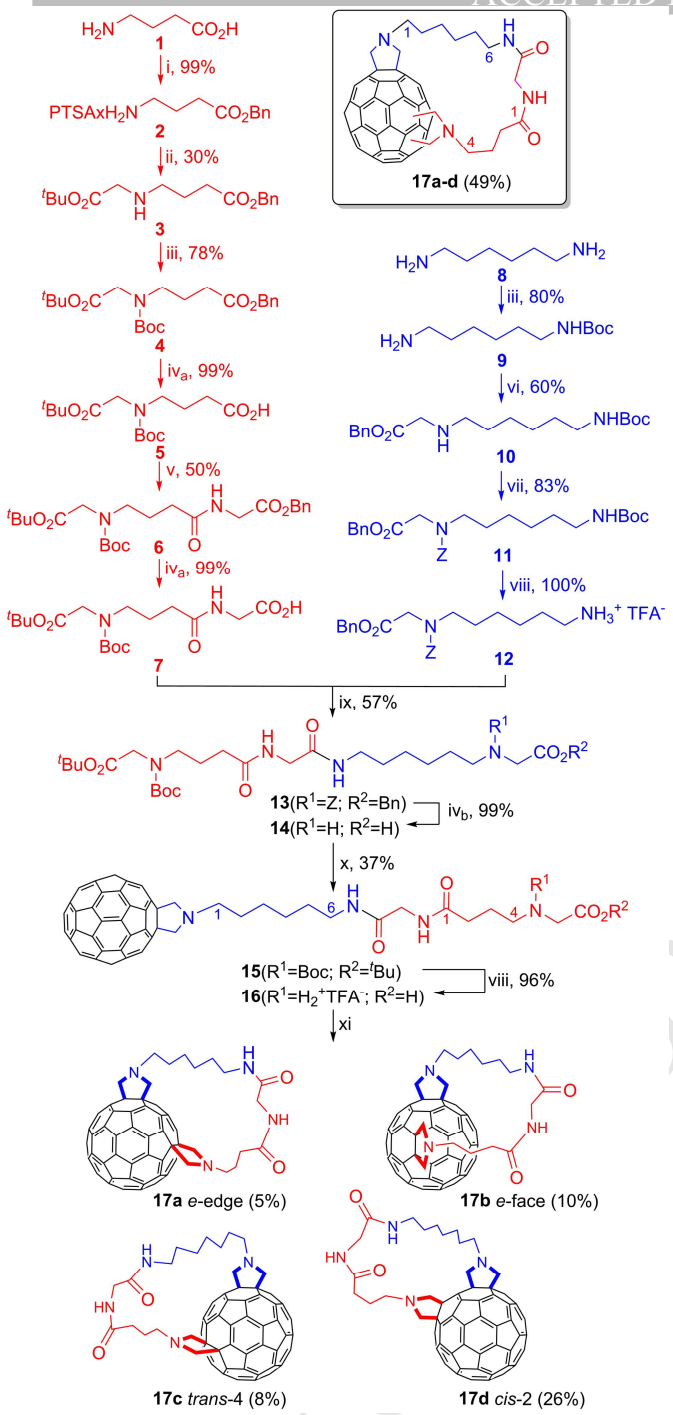

Scheme 1: Multistep synthetic route towards bis(pyrrolidino)fullerenes **17** starting from GABA **1** and 1,6-hexanediamine **8**: (i) BnOH, PTSAxH_2O, PhMe, reflux, 5 h; (ii) $NaHCO_3$; $^tBuO_2CCH_2Br$, Et_3N, CH_2Cl_2, 0 ºC, 5 h; (iii) Boc_2O, $CHCl_3$, 0 °C→r.t., 24 h; (iv) (a) H_2, Pd/C, MeOH, r.t.: 1 h, (b) 24h; (v) Et_3N, DCC, DMAP, CH_2Cl_2, GlyOBn, r.t., 24 h; (vi) BnO_2CCH_2Br, CH_2Cl_2, 0 °C→r.t., 24 h; (vii) ZCl, Et_3N, CH_2Cl_2, 0 °C→ r.t., 4 h; (viii) TFA, CH_2Cl_2, r.t., 24 h; (ix) Et_3N, DCC, DMAP, CH_2Cl_2, 0 °C→r.t., 24 h; (x) C_{60}, HCHO, PhMe, reflux, 1 h; (xi) Et_3N, PhMe, HCHO, reflux, 4 h.

phenyl-C_{61}-butyric acid methyl ester using a tether-directed 1,3-dipolar cycloaddition of azomethine ylides was reported by Zhang and co-workers.[8]

The selectivity of a double Prato cycloaddition of C_{2v}-symmetric diglycine substrates as reactive centers linked by flexible alkyl[12] or polyoxamethylene[13] tethers to the fullerene C_{60} was recently examined in our research group. The results showed that the regioselectivity of a one-pot biscycloaddition of the investigated flexible substrates on fullerene is significantly improved, giving mostly mixtures of *cis*-regioisomers with the exception of dodecamethylene- and trioxatridecamethylene-tethers which additionally give *trans*-4 and/or *equatorial* isomers.

Here we report the regioselective synthesis of four bis(pyrrolidino)fullerenes possessing an asymmetric macrocyclic diamide tether, using a two-step Prato monoaddition reaction sequence, and their complete spectral and self-assembly characterization. Also, we describe the multistep preparation of a reactive diglycine substrate comprised of the non-symmetric diamide tether with hexamethylene, Gly and GABA (4-aminobutanoic acid) subunits.

2. Results and Discussion

In order to investigate the regiochemical outcome of the Prato reaction in the synthesis of bridged bisadducts via a fullerene monoaduct, as well as the tether directing ability, we designed the new tether substrate **14** in which the reactive glycine and protected glycinate termini were bridged by an unsymmetrical, semi-flexible subunit consisting of 14 atoms. As has been mentioned before, previous research showed that flexible tethers favored *cis*-addition patterns, while the bridge prolongation allowed formation of *equatorial* and *trans*-isomers. Also, an introduction of heteroatom (oxygen) into the linker led to the prevalence of the *cis*-2 isomer. So, we supposed that the incorporation of a diamide segment would additionally increase the rigidity of the tether, while the presence of appropriate alkyl moieties would allow the formation of more distant addition patterns. At the same time, employing alkyl segments of the different lengths would give a possibility to distinguish both equatorial positions (*e*-edge and *e*-face). Based on that, the tether containing HO-Gly-C6-diamide(Gly)-C4-GlyOtBu sequence seemed reasonable. As summarized in Scheme 1, the tether **14** was transformed to the fullerene monoadduct **15**, and after deprotection of the glycinate, subjected to the second (intramolecular) cycloaddition affording four bisadducts **17a-d**.

The key intermediates **7** and **12** were synthesized from commercially available 4-aminobutanoic acid (GABA, **1**) and 1,6-hexanediamine **8** in overall yields of 11% and 40%, respectively (for experimental details and spectral characterization of compounds **2**-**7** and **9**-**14** see SI). GABA was esterified with benzyl alcohol in the presence of *p*-toluenesulfonic acid monohydrate (PTSA) in almost quantitative yield (99%) giving the corresponding benzyl ester in the form of the PTSA salt **2**. The benzyl ester **2** was alkylated with *tert*-butyl bromoacetate (TBBA) to afford the glycine *tert*-butyl ester **3** in 30% yield. The secondary amino group in **3** was protected with di-*tert*-butyl carbamate (Boc_2O) giving compound **4** in 78% yield. Palladium-catalyzed hydrogenolysis of the benzyl ester group gave acid **5** (99%). DCC/DMAP-mediated amide coupling of the obtained acid **5** and glycine benzyl ester (GlyOBn) afforded the corresponding amide **6** in 50% yield. In the next step the benzyl group of **6** was removed by catalytic hydrogenolysis giving acid **7** in nearly quantitative yield.

The TFA salt of amine **12** was prepared from diamine **8** in four steps in an overall yield of 40% (mono-NH-Boc-protection, N-alkylation of **9** with benzyl bromoacetate (BBA), Z-protection of NH group in **10**, and TFA-mediated deprotection of NH-Boc group of **11**). Release of the free amine from **12** followed by coupling with acid **7** by a standard DCC/DMAP procedure afforded diamide **13** in 57% yield. The benzyloxycarbonyl- and benzyl groups were cleaved by catalytic hydrogenolysis to provide the amino acid **14** in 99% yield. This α-amino acid was

allowed to react with paraformaldehyde and C_{60} under Prato conditions in refluxing toluene for 1 h to form the double-protected fulleropyrrolidine derivative **15** in 37% yield. Finally, the ammonium trifluoroacetate salt **16** was obtained in nearly quantitative yield after deprotection of **15** by using TFA in CH_2Cl_2. In the last step of the synthesis, in situ-liberated amino acid of **16** in the presence of a fivefold excess of paraformaldehyde reacted in refluxing toluene for 4 h, affording a mixture of four regioisomers (**17a-d)** in a yield of 49%. The crude mixture of regiosomers was purified by dry-flash column chromatography on silica gel using toluene/ethyl-acetate/methanol mixtures to elute as the first fraction, the *e*-edge regioisomer **17a** in 5% yield, followed by the second equatorial, *e*-face regioisomer **17b** in 10% yield, *trans*-4 regioisomer **17c** in 8% yield, and finally *cis*-2 bisadduct **17d**, as the main regioisomer, in 26% yield. The relative ratio of the isolated regioisomeric bisadducts *e*-edge/*e*-face/*trans*-4/*cis*-2 was 1.0:1.9:1.5:4.9. Comparative analysis of the ratio of the obtained bisadduct regioisomers **17** with those in recently synthesized bisadducts in two series with flexible tethers of a similar length (dodecamethylene[12] and trioxatridecamethylene-tethered substrates[13]) revealed a dependence of the regioselectivity on the tether structure. Table 1 illustrates a comparison of their regioselectivity with various distribution of *cis*-, *equatorial* and *trans*-4 regioisomers and better regioselectivity of the investigated cycloaddition reaction relative to bisadducts prepared using Prato biscycloaddition with a polyoxa-tethered bisglycine derivative. The increased ratio for the *cis*-2 isomers is observed for the bisadducts with polyoxa and peptide tethers while the *trans*-4 is the preferred regioisomer with the alkyl tether.

It could be suggested that the tether rigidity, resulting from the presence of the intramolecular hydrogen bond in the diamide fragment, played a role in the regiochemical outcome of the second cycloaddition and preferable formation of the *cis*-2 product **17d**. In addition, the selectivity of the second cycloaddition toward functionalized vs. non-functionalized fullerene (i.e. formation of bisadducts vs. bridged difullerene compound) was also examined. To that purpose, the fullerene monoadduct **16** was treated with an excess of the C_{60} (2, 5 and 10 mol equivalents) under standard reaction conditions. In all experiments only the mixture of bisadducts **17**, with no alteration in the products distribution was formed, while the C_{60} dumbbell molecule was not detected. The absence of the difullerene compound also support the importance of the hydrogen bond anchored, bent conformation of the tether.

Table 1. Comparison of relative distribution of the isolated regioisomeric bisadducts of fullerene containing alkyl,[12] polyoxa,[13] and diamide tethers.

Tether	**Ratio** *cis*-1:*cis*-2:*cis*-3:*eq*:*trans*-4
-$(CH_2)_{12}$-	0:1.0:0:1.0:2.8
-$(CH_2)_3O(CH_2)_2O(CH_2)_2O(CH_2)_3$-	1.0:4.8:2.8:1.3:0
-$(CH_2)_6NHCOCH_2NHCO(CH_2)_3$-	0:4.9:0:2.9(1.0:1.9)[a]:1.5

[a] the *e*-edge:*e*-face ratio

Monoadduct **15** and bisadducts **17a-d** were fully characterized by UV-vis spectrophotometry, 1D and 2D NMR spectroscopy and high-resolution mass spectrometry (see Experimental part and SI). All fullerene bisadducts gave the expected protonated molecular ion peak $(M+H)^+$, as well as $(M+2H)^{2+}$ peak in their ESI-TOF-MS spectra (SI). The addition patterns were confirmed by comparison with the UV/Vis absorption spectra of previously reported bispyrrolidinofullerenes bridged by flexible alkyl- and polyoxamethylene-tethers.[12,13] According to the number of ^{13}C signals and their intensities, the isomers **17a** and **17b** are symmetric, matching the *Cs*- symmetry of the equatorial bisaddition patterns, *e*-edge and *e*-face, respectively, while the regioisomers **17c** and **17d** are asymmetric. The ^{13}C NMR spectra of the two equatorial isomers showed 29 fullerene sp^2 resonances, two of which have half-intensity, indicating their *Cs* symmetry (SI, Figures S63 and S71). The sp^3 fullerene C atoms located on the mirror plane gave two half-intensity signals at about 70 ppm (δ 69.44, 69.9 ppm for **17a** and 69.44, 69.73 ppm

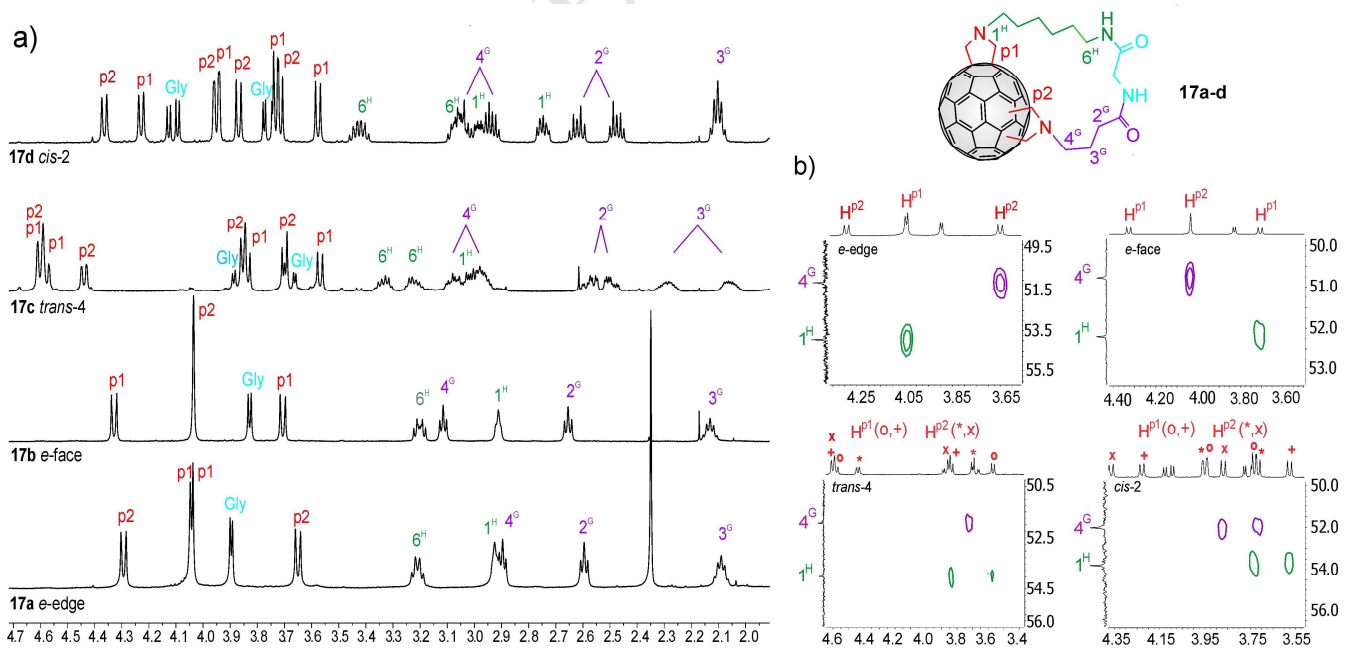

Figure 1. a) Expanded parts of ^1H NMR spectra of bisadduct regioisomers **17a** (*e*-edge), **17b** (*e*-face), **17c** (*trans*-4) and **17d** (*cis*-2); b) Important HMBC correlations of the pyrrolidine protons (H^p) with C atoms in the tether ($C(4)^{GABA}$ or $C(1)^{hexyl}$) in *e*-edge, *e*-face, *trans*-4 and *cis*-2 regioisomers. Peaks associated with: pyrrolidine methylene protons are labeled p1 (next to the hexyl-group) and p2 (next to the GABA unit), GABA and hexyl methylene protons and carbons are labeled G and H.

for **17b**) and one full-intensity signal centered at 69.57 (**17a**) and 70.22 ppm (**17b**) for the remaining two sp^3 fullerene C atoms. Also, the pyrrolidine methylene C atoms gave three signals, two half-intensity at δ ~ 65 and 68 ppm and one full-intensity signal at δ ~ 67 ppm (SI, Table S1). Characteristic sp^2 C fullerene signals of *trans*-4 (50 signals) and *cis*-2 bisadducts (47 signals) as well as eight signals of sp^3 fullerenic and pyrrolidinic carbon atoms are observed in the ranges of δ 130-160 and 65-70 ppm, respectively, strongly suggesting molecular asymmetry. Additionally, ten C atoms of the tether (N-$(CH_2)_6$-NHCO-CH_2-NHCO-$(CH_2)_3$-N) in all four regioisomers gave 10 signals corresponding to the hexyl, Gly and GABA methylene units in the aliphatic δ 22-54 ppm region of the ^{13}C NMR spectra, as well as two signals for the Gly and GABA amide carbonyl atoms at δ ~168 and 173 ppm, respectively (SI, Table and Figures S63, S71, S80 and S89).

Figure 1 displays parts of the ^1H NMR spectra (a) and important HMBC correlations (b) of bisadducts **17**. The ^1H NMR spectra of equatorial isomers **17a,b** (SI: Figures S62 and S70) contain two doublets (2H each) of different chemical shifts at δ ~ 3.7 and 4.3 ppm for the pyrrolidine protons belonging to the ring perpendicular to the plane of symmetry, and one (4H) or two (2H each) singlets (δ 4.04 ppm for **17b**; 4.04 and 4.05 ppm for **17a**) for CH_2 protons of the pyrrolidinic ring which lies in the plane of symmetry, indicating their equivalence in **17b**, as well as their non-equivalence in regioisomer **17a**. In addition, their ^1H NMR spectra showed signals corresponding to the Gly methylene protons centered at δ 3.90 and 3.83 ppm, terminal methylene protons of the hexamethylene unit at δ 3.2 (6^H) and 2.9 ppm (1^H), and the GABA methylene protons at δ ~ 2.1 (triplet, 3^G), and 2.6 ppm (quintet, 2^G), with slight chemical shift differences, as well as triplet signals for the GABA methylene protons next to the pyrrolidine ring at δ 2.90/3.20 ppm (4^G), with the biggest chemical shift difference (Δδ=0.22 ppm). The broad triplet resonances at δ 5.61 and 5.65 ppm (NH^{hexyl}), and 6.85 and 7.20 ppm (NH^{Gly}) corresponded to the exchangeable amide protons in **17a** and **17b**, respectively.

In the ^1H NMR spectra of bisadducts **17c** (*trans*-4) (SI: Figure S78) and **17d** (*cis*-2) (SI: Figure S88), the pyrrolidinic non-equivalent protons appeared as eight doublets in the region of 3.5-4.6 ppm (Figure 1a). The broad triplet resonances at δ 5.55 and 5.86 (NH^{hexyl}) and at δ 6.86 and 6.93 ppm (NH^{Gly}) correspond to the exchangeable amide protons for **17c** and **17d**, respectively. The methylene protons of the GABA and hexyl units have

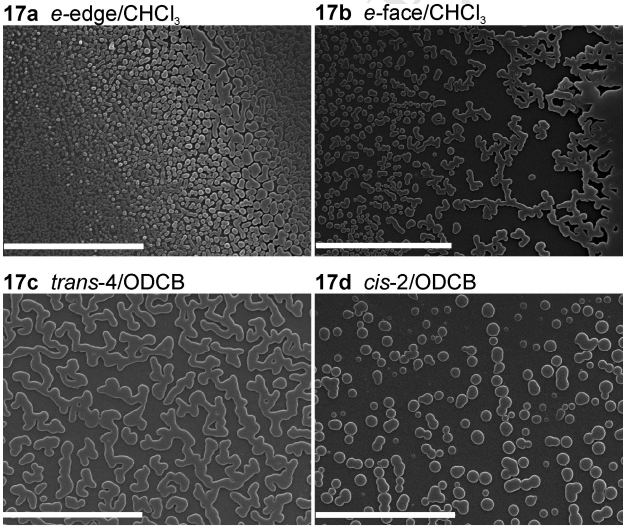

Figure 2. SEM images of nano- and microstructures obtained from bisadduct regioisomers **17**, upon evaporation from $CHCl_3$ (for **17a** and **17b**) and ODCB (for **17c** and **17d**) solutions deposited on glass substrate at room temperature. Scale bars correspond to 10 μm.

different chemical shifts in the 2.0 to 3.5 ppm region of the ^1H NMR spectra. Also, glycine methylene protons gave two dd signals in the range of 3.6-4.15 ppm. Separated resonances additionally confirm different environments to the methylene protons above the fullerene sphere. The important HMBC three-bond correlations from pyrrolidine protons (H^p) to the terminal carbons of the tether ($C(4)^{GABA}$ and $C(1)^{hexyl}$) observed in all four regioisomers was used for determination of the protons of the pyrrolidine rings next to the hexamethylene and GABA moieties (H^{p1} and H^{p2}, respectively, Figure 1b).

Scanning electron microscopy (SEM) was used for the characterization and the morphological study of their self-assembled structures by a solution drop-drying method.[14] Bisadduct regioisomers **17** have two elements of ordering, the hydrophobic interactions of fullerene cages and the hydrophilic interactions between the amide groups. SEM analysis of PhMe and *o*-dichlorobenzene (ODCB) solutions of regioisomeric bisadducts **17** (Figure 2) revealed their affinity in the formation of spherical nano- and microstructures with a pronounced tendency for networking, similarly to the self-organized structures obtained from fullerene-peptide-steroid triads investigated in our research group.[15]

3. Conclusion

In summary, we report the regioselective stepwise synthesis of four macrocyclic bis(pyrrolidine) C_{60} adducts (*e*-edge, *e*-face, *trans*-4, and *cis*-2), and their complete spectral characterization. Also, we describe the multistep preparation of a diamide substrate containing two glycine substructures. Fullerene monoadduct and four bisadduct regioisomers, including both equatorial isomers, were isolated in pure form using dry-flash column chromatography without the use of high-performance liquid chromatography (HPLC) separation and purification, and were fully characterized. The aggregation properties of regioisomers **17** in $CHCl_3$ and ODCB solution were studied using SEM. The morphology results showed similarity in the formation of spherical assemblies and their merging and networking. These novel C_{60} regioisomers-fused macrocyclic lactams are expected to be potentially important as building blocks in the synthesis of higher fullerene adducts and complex supramolecular architectures.

4. Experimental section

4.1. General: Flash column chromatography (FCC) and dry-column flash chromatography (DCFC) were carried out with Merck silica gel 0.04–0.063 mm and 0.015-0.04 mm, respectively. Thin layer chromatography (TLC) was carried out on precoated silica gel 60 F_{254} plates. Melting points were determined on a Digital melting point WRS-1B apparatus and are uncorrected. IR spectra were recorded with a *Perkin-Elmer FTIR 1725X* spectrophotometer. UV spectra were recorded with a *GBC-Cintra 40* UV-vis spectrophotometer. ^1H- and ^{13}C NMR spectra were recorded with *Varian Gemini 200* (^1H at 200 MHz, ^{13}C at 50 MHz) and *Bruker Avance* spectrometers (^1H at 500 MHz, ^{13}C at 125 MHz). Chemical shifts are measured in ppm, *J* in Hz. The sample was dissolved in the indicated solvent system, and TMS was used as an internal reference. The homonuclear 2D (DQF-COSY) and the heteronuclear 2D ^1H-^{13}C spectra (HSQC, HMBC) were recorded with the usual settings. The NMR spectra of all carbamates (**4**−**7**, **11** and **12)** are consistent with the expected structure but are complicated (splitting of some signals) by the presence of carbamate rotamers. The high-resolution mass spectra were obtained with an *Agilent Technologies 6210* TOF LC-MS spectrometer. Investigations of sample morphology were carried out with SEM, using a JEOL JSM-840A instrument, at an

acceleration voltage of 30 kV. A drop of 1 mM solution of sample in $CHCl_3$ and ODCB was deposited on the surface of glass substrate and left for 24 h to slowly evaporate in a glass petri dish (diameter 10 cm) under a PhMe atmosphere at room temperature. The investigated samples were gold sputtered in a JFC 1100 ion sputterer and then subjected to SEM observations. The solvents used for the SEM experiments (HPLC grade) were stored over 3 Å molecular sieves and degassed under vacuum prior use.

4.2. Synthesis of fulleropyrrolidine 15. A suspension of glycine derivative **14** (72.5 mg, 0.14 mmol), C_{60} (98.4 mg, 0.014 mmol), and HCHO (21 mg, 0.70 mmol) in PhMe (100 mL) was heated under reflux for 1 h. The obtained reaction mixture was cooled to room temperature and evaporated to dryness. DCFC on SiO_2 using PhMe gave unreacted C_{60} (55 mg, 56%). Elution with PhMe/EtOAc/MeOH (5/5/1) and subsequent precipitation from a highly concentrated CH_2Cl_2 solution with MeOH gave pure fulleropeptide ester **15** (62.3 mg, 37%) as a brown powder. IR(ATR): 3344, 3057, 2978, 2934, 2861, 2796, 1744, 1691, 1545, 1462, 1430, 1368, 1253, 1159 cm^{-1}; ^1H NMR (500 MHz, $CDCl_3$): δ=7.00 (t, *J*=5.2 Hz, 1H, HN^{hexyl}), 6.66 (t, *J*=5.8 Hz, 1H, HN^{Gly}), 4.41 (s, 4H, H_2C^{pyrr}), 3.97 (d, *J*= 6.0 Hz, 2H, H_2C^{Gly}), 3.75 (s, 2H, $H_2C^{GlyOtBu}$), 3.35-3.31 (m, 4H, $H_2C(4)^{GABA}$, $H_2C(6)^{hexyl}$), 3.07 (t, *J*=7.5 Hz, 2H, $H_2C(1)^{hexyl}$), 2.35 (br t, *J*=6.5 Hz, 2H, $H_2C(2)^{GABA}$), 1.94 (app. quint, *J*=7.5 Hz, 2H, $H_2C(2)^{hexyl}$), 1.85 (app. quint, *J*=6.0 Hz, 2H, $H_2C(3)^{GABA}$), 1.68-1.60 (m, 4H, $H_2C(3, 5)^{hexyl}$), 1.55-1.48 (m, 2H, $H_2C(4)^{hexyl}$), 1.47 (s, 9H, H_3C), 1.46 (s, 9H, H_3C) ppm; ^{13}C NMR (500 MHz, $CDCl_3$): δ=173.38 (CO^{GABA}), 169.33 (CO^{Gly}), 169.09 ($CO_2{}^t$Bu), 156.26 (CO^{Boc}), 155.15, 147.30, 146.23, 146.11, 146.05, 145.70, 145.39, 145.28, 144.56, 143.09, 142.61, 142.25, 142.06, 141.88, 140.14, 136.23 (sp^2-C^{full}), 81.64, 80.45 (C^{tBu}), 70.69 (sp^3-C^{full}), 68.03 (CH_2^{pyrr}), 55.00 ($CH_2(1)^{hexyl}$), 50.29 (CH_2CO_2tBu), 47.11 ($CH_2(4)^{GABA}$), 43.74 (CH_2^{Gly}), 39.51 ($CH_2(6)^{hexyl}$), 32.83 ($CH_2(2)^{GABA}$), 29.58 ($CH_2(5)^{hexyl}$), 28.79 ($CH_2(2)^{hexyl}$), 28.26 (CH_3), 28.07 (CH_3), 27.34 ($CH_2(3)^{hexyl}$), 26.88 ($CH_2(4)^{hexyl}$), 24.30 ($CH_2(3)^{GABA}$) ppm; UV/Vis (CH_2Cl_2): $\lambda_{max}(\varepsilon)$ = 254 (29000), 306 (31000), 327 (31000), 431 (6900), 698 (2100) nm ($mol^{-1}dm^3cm^{-1}$); MS(ESI): Calcd for $C_{85}H_{47}N_4O_6$ $(M+H)^+$: 1219.3490, found 1219.3498.

4.3. Deprotection of fulleropyrrolidine 15. A solution of fullerene derivative **15** (60 mg, 0.049 mmol) in TFA/DCM (1:1, 4 mL) was stirred at room temperature for 24 h and then evaporated to dryness. The excess of TFA was removed by co-evaporation with PhMe (3×10 mL), giving the corresponding TFA salt **16** (55.8 mg, 96.3%), as a brown powder, which was used in the next step without further purification.

IR: 3700-2300 (broad band), 3302, 2924, 2853, 1674, 1427, 1199, 1136 cm^{-1}; UV (DCM): λ_{max}: 220-300, 429, 538, 702 nm. MS(ESI): Calcd for $C_{76}H_{31}N_4O_4$ $(M)^+$: 1063.2340, found 1063.2325.

4.4. Synthesis of bis(pyrrolidino)fullerenes 17a-d. To a solution of the TFA salt **16** (97.2 mg, 0.087 mmol) in PhMe (100 mL), Et_3N (0.2 mL) was added and the mixture was stirred at room temperature for 30 min. Then HCHO (13 mg, 0.43 mmol, 5 equiv.) was added and the mixture heated to reflux for 4 h. The obtained reaction mixture was cooled to room temperature and separated by DCFC. Regioisomeric bisadducts **17** were eluted in the following order: *e*-edge, *e*-face, *trans*-4, *cis*-2. DCFC (with preparative TLC for *trans*-4) and further precipitation of crude products from their highly concentrated CH_2Cl_2 solutions with MeOH yielded: *e*-edge bisadduct **17a** (4.8 mg, 5.3%, DCFC: PhMe/EtOAc/MeOH 5:5:0.1), *e*-face bisadduct **17b** (8.9 mg, 9.9%, DCFC: PhMe/EtOAc/MeOH 5:5:0.1), *trans*-4 bisadduct **17c** (7.2 mg, 8.0%, DCFC: PhMe/EtOAc/MeOH 5:5:0.15; TLC: $CHCl_3$/MeOH 100:3), and *cis*-2 bisadduct **17d** (23.3 mg, 26.0%, DCFC: PhMe/EtOAc/MeOH 5:5:0.2). Total yield of the isolated bisadducts was 49.2% (*e*-edge/e-face/*trans*-4/*cis*-2 = 1:1.9:1.5:4.9).

4.4.1. Bisadduct 17a (*e*-edge): IR(ATR): 3395, 3296, 2926, 2858, 2782, 1650, 1512, 1456, 1341, 1261, 1119 cm^{-1}; ^1H NMR (500 MHz, $CDCl_3$): 6.85 (br s, 1H, NH^{Gly}), 5.61 (br d, 1H, NH^{hexyl}), 4.29 (d, *J*=9.6 Hz, 2H, HC^{pyrr-2}), 4.05 (s, 2H, H_2C^{pyrr-1}), 4.04 (s, 2H, H_2C^{pyrr-1}), 3.90 (d, *J*=4.4 Hz, 2H, H_2C^{Gly}), 3.65 (d, *J*=9.6 Hz, 2H, HC^{pyrr-2}), 3.21 (q, *J*=7.0 Hz, 2H, $H_2C(6)^{hexyl}$), 2.92 (br s, 2H, $H_2C(1)^{hexyl}$), 2.90 (t, *J*=6.0 Hz, 2H, $H_2C(4)^{GABA}$), 2.60 (t, *J*=6.0 Hz, 2H, $H_2C(2)^{GABA}$), 2.09 (quint, *J*=6.0 Hz, 2H, $H_2C(3)^{GABA}$), 1.82-1.72 (m, 4H, $H_2C(2)^{hexyl}$, $H_2C(4)^{hexyl}$), 1.62-1.56 (m, 2H, $H_2C(5)^{hexyl}$), 1.50-1.43 (m, 2H, $H_2C(3)^{hexyl}$) ppm; ^{13}C NMR (125 MHz, $CDCl_3$): 172.84 (CO^{GABA}), 167.64 (CO^{Gly}), 159.52, 153.77, 153.30, 152.31, 149.64, 148.80, 148.12, 147.69, 147.51, 147.38, 147.24, 145.87, 145.71, 145.13, 145.01, 144.55, 144.35, 143.59, 143.34, 142.29, 141.52, 141.45, 141.16, 140.97, 139.51, 136.61, 135.42 (sp^2 C^{full}), 69.90 (1C, sp^3 C^{full}), 69.57 (2C, sp^3 C^{full}), 69.44 (1C, sp^3 C^{full}), 68.46 (CH_2^{pyrr-1}), 67.10 ($2CH_2^{pyrr-2}$), 65.02 (CH_2^{pyrr-1}), 53.95 ($CH_2(1)^{hexyl}$), 51.13 ($CH_2(4)^{GABA}$), 42.51 (CH_2^{Gly})), 38.27 ($CH_2(6)^{hexyl}$), 33.17 ($CH_2(2)^{GABA}$), 28.11 ($CH_2(5)^{hexyl}$), 27.08 ($CH_2(4)^{hexyl}$), 25.11 ($CH_2(3)^{hexyl}$), 24.47 ($CH_2(2)^{hexyl}$), 23.36 ($CH_2(3)^{GABA}$) ppm; Key HMBC correlations: 3.65d/51.13 (H^{pyrr-2}/$C(4)^{GABA}$), 4.05s and 4.04s/53.95 (H^{pyrr-1}/$C(1)^{hexyl}$); MS (ESI): Calculated for $C_{76}H_{32}N_4O_2$ $(M+2H)^{2+}$: 516.1257, $(M+H)^+$: 1031.2442, found 516.1265, 1031.2482; UV (CH_2Cl_2): $\lambda_{max}(\varepsilon)$: 316 (7800), 422 (1100) nm ($mol^{-1}dm^3cm^{-1}$).

4.4.2. Bisadduct 17b (*e*-face): IR(ATR): 3317, 2928, 2856, 2793, 1654, 1523, 1455, 1340, 1262, 1160 cm^{-1}; ^1H NMR (500 MHz, $CDCl_3$): 7.20 (br t, *J*=5.5 Hz, 1H, NH^{Gly}), 5.65 (br t, *J*=5.5 Hz, 1H, NH^{hexyl}), 4.33 (d, *J*=9.5 Hz, 2H, HC^{pyrr-1}), 4.04 (s, 4H, H_2C^{pyrr-2}), 3.83 (d, *J*=5.5 Hz, 2H, H_2C^{Gly}), 3.71 (d, *J*=9.5 Hz, 2H, HC^{pyrr-1}), 3.20 (dt, *J*=10.0, 5.5 Hz, 2H, $H_2C(6)^{hexyl}$), 3.12 (t, *J*=6.0 Hz, 2H, $H_2C(4)^{GABA}$), 2.91 (br s, 2H, $H_2C(1)^{hexyl}$), 2.65 (t, *J*=6.5 Hz, 2H, $H_2C(2)^{GABA}$), 2.13 (quint, *J*=6.5 Hz, 2H, $H_2C(3)^{GABA}$), 1.72-1.66 (m, 4H, $H_2C(2)^{hexyl}$, $H_2C(3)^{hexyl}$), 1.56-1.50 (m, 2H, $H_2C(5)^{hexyl}$), 1.42 (t, *J*=6.5 Hz, 2H, $H_2C(4)^{hexyl}$) ppm; ^{13}C NMR (125 MHz, $CDCl_3$): 173.77 (CO^{GABA}), 168.59 (CO^{Gly}), 159.09, 154.55, 153.24, 152.56, 149.71, 148.88, 148.14, 147.76, 147.59, 147.49, 147.24, 146.12, 145.81, 145.21, 145.03, 144.70, 144.65, 144.39, 143.62, 143.29, 142.31, 141.65, 141.29, 141.23, 140.79, 139.13, 136.67, 135.67 (sp^2 C^{full}), 70.22 (2C, sp^3 C^{full}), 69.73 (1C, sp^3 C^{full}), 69.44 (1C, sp^3 C^{full}), 67.53 (CH_2^{pyrr-2}), 66.92 ($2CH_2^{pyrr-1}$), 65.37 (CH_2^{pyrr-2}), 52.21 ($CH_2(1)^{hexyl}$), 50.77 ($CH_2(4)^{GABA}$), 42.76 (CH_2^{Gly})), 39.85 ($CH_2(6)^{hexyl}$), 33.54 ($CH_2(2)^{GABA}$), 29.62 ($CH_2(5)^{hexyl}$), 27.56 ($CH_2(3)^{hexyl}$), 26.22 ($CH_2(4)^{hexyl}$), 25.95 ($CH_2(2)^{hexyl}$), 23.82 ($CH_2(3)^{GABA}$) ppm; Key HMBC correlations: 4.04s/50.77 (H^{pyrr-2}/$C(4)^{GABA}$), 3.71d/52.21(H^{pyrr-1}/$C(6)^{hexyl}$); MS (ESI): Calculated for $C_{76}H_{32}N_4O_2$ $(M+2H)^{2+}$: 516.1257, $(M+H)^+$: 1031.2442, found 516.1253, 1031.2424; UV (CH_2Cl_2): $\lambda_{max}(\varepsilon)$: 314 (8200), 422 (1100) nm ($mol^{-1}dm^3cm^{-1}$).

4.4.3. Bisadduct 17c (*trans*-4): IR(ATR): 3318, 2927, 2856, 2794, 1649, 1523, 1453, 1340, 1260, 1156 cm^{-1}; ^1H NMR (500 MHz, $CDCl_3$): 6.86 (t, *J*=4.8 Hz, 1H, NH^{Gly}), 5.60 (t, *J*=5.5 Hz, 1H, NH^{hexyl}), 4.60 (br d, *J*=9.5 Hz, 2H, HC^{pyrr-1}, HC^{pyrr-2}), 4.58 (d, *J*=9.5 Hz, 1H, HC^{pyrr-1}), 4.44 (br d, *J*=9.0 Hz Hz, 1H, HC^{pyrr-2}), 3.90-3.84 (m, 1H, H_2C^{Gly}), 3.85 (d, *J*=9.0 Hz, 1H, HC^{pyrr-2}), 3.84 (d, *J*=9.0 Hz, 1H, HC^{pyrr-1}), 3.70 (d, *J*=9.0 Hz, 1H, HC^{pyrr-2}), 3.70-3.64 (m, 1H, H_2C^{Gly}), 3.57 (d, *J*=9.0 Hz, 1H, HC^{pyrr-1}), 3.38-3.29 (m, 1H, $HC(6)^{hexyl}$), 3.26-3.19 (m, 1H, $HC(6)^{hexyl}$), 3.11-3.05 (m, 1H, $HC(4)^{GABA}$), 3.04-2.98 (m, 2H, $H_2C(1)^{hexyl}$), 3.00-2.93 (m, 1H, $HC(4)^{GABA}$), 2.61-2.46 (m, 2H, $H_2C(2)^{GABA}$), 2.34-2.24 (m,

1H, HC(3)^{GABA}), 2.10-2.01 (m, 1H, HC(3)^{GABA}), 1.92-1.72 (m, 4H, $H_2C(2)^{hexyl}$, $H_2C(3)^{hexyl}$), 1.61-1.50 (m, 4H, $CH_2(5)^{hexyl}$, $CH_2(4)^{hexyl}$) ppm; ^{13}C NMR (125 MHz, $CDCl_3$): 172.96 (CO^{GABA}), 168.19 (CO^{Gly}), 154.11, 153.76, 153.47, 153.37, 152.31, 151.84, 150.86, 150.12, 150.04, 149.46, 149.16, 148.58, 148.48, 148.38, 148.15, 147.39, 147.29, 147.06, 146.99, 146.26, 146.12, 146.07, 145.74, 145.63, 144.59, 144.53, 144.35, 142.80, 142.53, 142.49, 142.45, 142.28, 141.92, 141.53, 141.48, 141.44, 141.38, 141.33, 138.91, 138.46, 136.04, 135.84, 135.33, 135.22, 131.33, 131.24 (sp^2 C^{full}), 69.80, 69.41, 69.24, 69.17 (sp^3 C^{full}), 68.50(CH_2^{pyrr-1}), 67.62(CH_2^{pyrr-2}), 67.07(CH_2^{pyrr-2}), 66.69 (CH_2^{pyrr-1}), 54.00 ($CH_2(1)^{hexyl}$), 51.93 ($CH_2(4)^{GABA}$), 43.13 (CH_2^{Gly}), 39.23 ($CH_2(6)^{hexyl}$), 34.75 ($CH_2(2)^{GABA}$), 29.35 ($CH_2(5)^{hexyl}$), 27.06 ($CH_2(2)^{hexyl}$), 26.24 ($CH_2(3)^{hexyl}$), 25.47 ($CH_2(4)^{hexyl}$), 22.80 ($CH_2(3)^{GABA}$) ppm; Key HMBC correlations: 3.70d/51.93 (H^{pyrr-2}/$C(4)^{GABA}$), 3.57d; 3.84d/54.00 (H^{pyrr-1}/$C(1)^{hexyl}$); MS (ESI): Calculated for $C_{76}H_{32}N_4O_2$ $(M+2H)^{2+}$: 516.1257, $(M+H)^+$: 1031.2442, found 516.1254, 1031.2438; UV (CH_2Cl_2): $\lambda_{max}(\varepsilon)$: 264 (35000), 308 (18000), 638 (290), 705 (200) nm ($mol^{-1}dm^3cm^{-1}$).

4.4.4. Bisadduct 17d (*cis*-2): IR(ATR): 3308, 2930, 2858, 2788, 1656, 1531, 1449, 1343, 1237, 1163, 1116 cm^{-1}; ^{1}H NMR (500 MHz, $CDCl_3$): 6.93 (t, *J*=5.2 Hz, 1H, NH^{Gly}), 6.00 (t, *J*=6.0 Hz, 1H, NH^{hexyl}), 4.36 (d, *J*=9 Hz, 1H, HC^{pyrr-2}), 4.23 (d, *J*=8.5 Hz, 1H, HC^{pyrr-1}), 4.11 (dd, *J*=6.5 Hz, 16.5 Hz, 1H, HC^{Gly}), 3.96 (d, *J*=9.0 Hz, 1H, HC^{pyrr-2}), 3.95 (d, *J*=9.0 Hz, 1H, HC^{pyrr-1}), 3.87 (d, *J*=9.0 Hz, 1H, HC^{pyrr-2}), 3.76 (dd, *J*=4.0; 16.0 Hz, 1H, HC^{Gly}), 3.73 (d, 1H, *J*=9.0 Hz, HC^{pyrr-1}), 3.72 (d, *J*=9.0 Hz, 1H, HC^{pyrr-2}), 3.58 (d, *J*=9.0 Hz, 1H, HC^{pyrr-1}), 3.47-3.38 (m, 1H, $HC(6)^{hexyl}$), 3.10-3.01 (m, 2H, $HC(6)^{hexyl}$, $HC(4)^{GABA}$), 3.01-2.96 (m, 1H, $HC(1)^{hexyl}$), 2.96-2.90 (m, 1H, $HC(4)^{GABA}$), 2.78-2.71 (m, 1H, $HC(1)^{hexyl}$), 2.62 (dt, *J*=13.5, 7.0 Hz, 1H, $HC(2)^{GABA}$), 2.47 (dt, *J*=13.5, 6.0 Hz, 1H, $HC(2)^{GABA}$), 2.10 (quint, *J*=6.5 Hz, 2H, $H_2C(3)^{GABA}$), 1.93-1.83 (m, 1H, $HC(2)^{hexyl}$), 1.82-1.74 (m, 1H, $HC(3)^{hexyl}$), 1.74-1.67 (m, 1H, $HC(2)^{hexyl}$), 1.67-1.61 (m, 2H, $H_2C(5)^{hexyl}$), 1.57-1.42 (m, 3H, $HC(3)^{hexyl}$, $H_2C(4)^{hexyl}$) ppm; ^{13}C NMR (125 MHz, $CDCl_3$): 173.72 (CO^{GABA}), 168.72 (CO^{Gly}), 158.61, 158.37, 156.76, 156.59, 149.32, 148.85, 148.77, 148.38, 148.01, 147.93, 147.87, 147.54, 147.47, 147.20, 147.16, 146.99, 146.91, 146.49, 146.14, 146.10, 145.82, 145.73, 145.54, 145.43, 145.13, 145.12, 144.89, 144.64, 144.55, 144.53, 144.22, 144.03, 142.92, 141.70, 141.65, 140.99, 139.09, 138.88, 133.90, 133.38, 133.26, 132.80, 129.18 (sp^2 C^{full}), 67.98 (CH_2^{pyrr-2}), 67.77 (CH_2^{pyrr-1}), 67.14, 66.95, 66.74, 66.68 (sp^3 C^{full}), 66.52 (CH_2^{pyrr-1}), 65.88 (CH_2^{pyrr-2}), 53.81 ($CH_2(1)^{hexyl}$), 52.02 ($CH_2(4)^{GABA}$), 43.30 (CH_2^{Gly})), 39.36 ($CH_2(6)^{hexyl}$), 33.86 ($CH_2(2)^{GABA}$), 28.15 ($CH_2(5)^{hexyl}$), 26.85 ($CH_2(2)^{hexyl}$), 25.39 ($CH_2(4)^{hexyl}$), 25.21 ($CH_2(3)^{hexyl}$), 24.28 ($CH_2(3)^{GABA}$) ppm; Key HMBC correlations: 3.73d/53.81 (H^{pyrr-1}/$C(1)^{hexyl}$), 3.57d/53.81 (H^{pyrr-1}/$C(1)^{hexyl}$), 3.87d/52.02 (H^{pyrr-2}/$C(4)^{GABA}$), 3.72d/52.01 (H^{pyrr-2}/$C(4)^{GABA}$); MS (ESI): Calculated for $C_{76}H_{32}N_4O_2$ $(M+2H)^{2+}$: 516.1257, $(M+H)^+$: 1031.2442, found 516.1254, 1031.2426; UV (CH_2Cl_2): $\lambda_{max}(\varepsilon)$: 259 (17000), 305 (8200), 446 (1000) nm ($mol^{-1}dm^3cm^{-1}$).

Acknowledgments

This research has been supported by Serbian Ministry of Education, Science and Technological Development, grant 172002.

References and notes

1. (a) Nakamura, Y.; Kato, S-I. *Chem. Rec.* **2011**, *11*, 77–94; (b) Zhou, Z.; Wilson, S. R. *Curr. Org. Chem.* **2005**, *9*, 789–811; (c) Hirsch, A. *Chem. Rec.* **2005**, *5*, 196–208; (d) Thilgen, C.; Sergeyev, S.; Diederich, F. *Top. Curr. Chem.* **2004**, *248*, 1–61; (e) Yau, H. C.; Bayazit, M. K.; Steinke, J. H. G.; Shaffer, M. S. P. *Macromolecules* **2014**, *47*, 4870–4875.
2. (a) Voroshazi, E.; Vasseur, K.; Aernouts, T.; Heremans, P.; Baumann, A.; Deibel, C.; Xue, X.; Herring, A.J.; Athans, A. J.; Lada, T. A.; Richter, H.; Rand, B. P. *J. Mater. Chem.* **2011**, *21*, 17345–17352; (b) Zhou, S.; Ouyang, J.; Golas, P.; Wang, F.; Pan, Y. *J. Phys. Chem. B* **2005**, *109*, 19741–19747.
3. (a) Beulen, M. W. J.; Rivera, J. A.; Herranz, M. A.; Illescas, B.; Martín, N.; Echegoyen, L. *J. Org. Chem.* **2001**, *66*, 4393–4398; (b) Lu, Q.; Schuster, D. I.; Wilson, S. R. *J. Org. Chem.* **1996**, *61*, 4764–4768; (c) Kordatos, K.; Bosi, S.; Da Ros, T.; Zambon, A.; Lucchini, V.; Prato, M. *J. Org. Chem.* **2001**, *66*, 2802–2808; (d) Djojo, F.; Herzog, A.; Lamparth, I.; Hampel, F.; Hirsch, A. *Chem. Eur. J.* **1996**, *2*, 1537–1547.
4. (a) Zhang, B.; Subbiah, J.; Lai, Y-Y.; White, J. M.; Jones, D. J.; Wong, W. W. H. *Chem. Commun.* **2015**, *51*, 9837–9840; (b) Tao, R.; Umeyama, T.; Higashino, T.; Koganezawa, T.; Imahori, H. *Chem. Commun.* **2015**, *51*, 8233–8236; (c) Meng, X.; Zhao, G.; Xu, Q.; Tan, Z.; Zhang, Z.; Jiang, L.; Shu, C.; Wang, C.; Li, Y. *Adv. Funct. Mater.* **2014**, *24*, 158–163.
5. Wilson, S. R.; Lu, Q. *Tetrahedron Lett*. **1995**, *36*, 5707–5710.
6. (a) Isaacs, L.; Haldimann, R. F.; Diederich, F. *Angew Chem Int Ed*. **1994**, *33*, 2339–2342; (b) Isaacs, L.; Diederich, F.; Haldimann, R. F. *Helv. Chim. Acta* **1997**, *80*, 317–342.
7. (a) Thilgen, C.; Diederich, F. *C. R. Chimie* **2006**, *9*, 868–880; (b) Sergeyev, S.; Schär, M.; Seiler, P.; Lukoyanova, E.; Echegoyen, L.; Diederich, F. *Chem. Eur. J.* **2005**, *11*, 2284–2294; (c) Nierengarten, J-F.; Gramlich, V.; Cardullo, F.; Diederich, F. *Angew. Chem., Int. Ed. Engl.* **1996**, *35*, 2101–2103; (d) Sutton, L. R.; Scheloske, M.; Pirner, K. S.; Hirsch, A.; Guldi, D. M.; Gisseelbrecht, J-P. *J. Am. Chem. Soc*. **2004**, *126*, 10370–10381; (e) Bourgeois, J-P.; Echegoyen, L.; Fibbioli, M.; Pretsch, E.; Diederich, F. *Angew. Chem., Int. Ed*. **1998**, *37*, 2118–2121.
8. Zhang, B.; White, J. M.; Jones, D. J.; Wong, W. W. H. *Org. Biomol. Chem*. **2015**, *13*, 10505–10510.
9. (a) Smith, P. M.; McCarty, A. L.; Nguyen, N. Y.; Zandler, M. E.; D'Souza, F. *Chem. Commun*. **2003**, 1754–1755; (b) Rotas, G.; Tagmatarchis, N. *Tetrahedron Lett.* **2009**, *50*, 398–401; (c) Iglesias, R. S.; Claessens, C. G.; Torres, T.; Rahman, G. M. A.; Guldi, D. M. *Chem. Commun*. **2005**, 2113–2115; (d) Zhou, Z.; Schuster, D. I.; Wilson, S. R. *J. Org. Chem.* **2006**, *71*, 1545–1551.
10. Chronakis, N.; Hirsch, A. *C. R. Chimie* **2006**, *9*, 862-867.
11. Bottari, G.; Trukhina, O.; Kahnt, A.; Frunzi, F.; Murata, Y.; Rodríguez-Fortea, A.; Poblet, J. M.; Guldi, D. M.; Torres, T. *Angew. Chem., Int. Ed*. **2016**, *55*, 11020–11025.
12. Kop, T.; Bjelaković, M.; Milić, D. *Tetrahedron* **2015**, *71*, 4801–4809.
13. Kop, T.; Bjelaković, M.; Đorđević, J.; Žekić, A.; Milić, D. *RSC Adv.* **2015**, *5*, 94599–94606.
14. (a) Babu, S. S.; Möhwald, H.; Nakanishi, T. *Chem. Soc. Rev.* **2010**, *39*, 4021–4035; (b) Guldi, D. M.; Zerbetto, F.; Georgakilas, V.; Prato, M. *Acc. Chem. Res.* **2005**, *38*, 38–43.
15. Bjelaković, M. S.; Kop, T. J.; Vlajić, M.; Đorđević, J.; Milić, D. R. *Tetrahedron* **2014**, *70*, 8564–8570.

Supplementary Material

Detailed reaction procedures for the syntheses of compounds **2-14** with their spectra, as well as Table S1 (NMR chemical shifts of bisadducts **17**) and spectra (IR, ^{1}H and ^{13}C NMR, COSY, HSQC, HMBC, MS, and UV-Vis) for fulleropyrrolidine monoadducts (**15** and **16)** and bisadducts (**17a-d)** are given in the Supplementary Information.